

DTIC FILE COPY

# Naval Ocean Research and Development Activity

July 1990

Report 247



## Investigations of Digital Image Analysis and Enhancements of GLORIA Acoustic Imagery

AD-A231 974

DTIC  
ELECTE  
FEB 25 1991  
S B D

K. B. Shaw  
C. L. Walker  
S. C. Lingsch  
Mapping, Charting, and Geodesy Division  
Ocean Science Directorate

F. A. Bowles  
P. Fleischer  
Seafloor Geosciences Division  
Ocean Science Directorate

## Foreword

The U.S. Navy is interested in improving underwater mapping and interpretation technologies for bottom and subbottom segmentation and classification, as well as feature extraction and identification of potential hazards. These refinements would greatly enhance the capability of Navy sensors and systems to distinguish and identify underwater objects and the geological structure of the bottom and subbottom.

The Naval Ocean Research and Development Activity was tasked to analyze imagery from the U.S. Geological Survey's Exclusive Economic Zone Survey Experiment. Digitally mosaicked GLORIA (Geological Long-Range Inclined Asdic) acoustic imagery were analyzed as a zeroth-order model for the acoustic imagery sensor, TAMU<sup>2</sup>, developed by Texas A&M University. Multiple image analysis techniques, as well as several image enhancement techniques, were applied to the data set.

This report describes the systems, the experiment, and the methods used to analyze the GLORIA data. Geological interpretations are also provided.

*W B Moseley*

**W. B. Moseley**  
Technical Director

*J B Tupaz*

**J. B. Tupaz, Captain, USN**  
Commanding Officer



Accession For	
NTIS GRA&I	<input checked="checked" type="checkbox"/>
DTIC TAB	<input type="checkbox"/>
Unannounced	<input type="checkbox"/>
Justification	
By	
Distribution/	
Availability Codes	
Dist	Avail and/or Special
A-1	

# Executive Summary

---

The Mapping, Charting, and Geodesy Division, Naval Ocean Research and Development Activity\*, was tasked to analyze imagery from the U.S. Geological Survey's Exclusive Economic Zone Survey Experiment. Digitally mosaicked GLORIA (Geological Long-Range Inclined Asdic) acoustic imagery were analyzed as a zeroth-order model for the acoustic imagery sensor, TAMU<sup>2</sup>, developed by Texas A&M University. Multiple image analysis techniques were applied to the data set, as well as several image enhancement techniques. Information gained from the analyses will be used in the exploitation of TAMU<sup>2</sup> imagery and bathymetry for U.S. Navy applications.

Technical attributes for acoustic imagery and bathymetric sensors used on current data-gathering systems were also studied and are described in the appendices.

This study led to the following conclusions.

- Improvements in digital mosaicking methods are of prime concern, as evidenced by the number of artifacts located in the USGS GLORIA mosaics.
- Histogram equalization yielded vastly improved GLORIA imagery, as far as preparing the imagery for feature extraction and for other forms of interpretation. However, the histogram equalization causes a nonlinear effect on texture application, which is important in segmenting acoustic imagery. This effect destroys the original texture content of the imagery.
- The probability distribution estimation was extremely close to Gaussian.
- Various-sized difference filters enhanced the bottom texture. The enhancement is useful for future segmentation and classification efforts with this type of imagery.
- A direct correlation between bathymetry and the acoustic imagery intensity profile could not be verified because severe mismatches were present in acoustic imagery resolution and the existing National Ocean Survey bathymetry: the correlation might not even exist.
- Image analysis offers powerful techniques for allowing a geologist or a geophysicist to interpret signatures and structures of the imagery. Histogram equalization, a nonlinear operation, utilizes the full bandwidth of the intensity range permitted for improved mudwave detection. The intensity profile technique allows the geologist a quantitative view of the intensity values along a vector. This type of view also improves mudwave pattern detection because the intensities fluctuate most in the mudwave area.
- Since GLORIA is a (approximately) 6.5-kHz sidescan, there are returns from the seafloor.

---

\*Recently designated the Naval Oceanographic and Atmospheric Research Laboratory.

---

- Kernel sizes for the various filtering techniques were found to be critical. The  $5 \times 5$  Gaussian filter provided enhancement of the darker relief areas.

- A  $5 \times 5$  median filter offered edge-sharpening without sacrificing image quality.

The analyses and conclusions led to these recommendations for study in the following areas.

- If a quantitative link between imagery intensity profiles and bathymetry could be established, then more information content could be extracted quantitatively from the acoustic imagery.

- The intensity profile would be even more useful in an automated scenario where the mudwave area detections would be performed without human interaction.

- Coregistered bathymetry and imagery are needed for optimum exploitation of bottom information. Statistical information for each pixel is required to develop confidence intervals for each bin of imagery and bathymetry. Both are designed into the new TAMU<sup>2</sup> system.

- Studies should be conducted with a functional TAMU<sup>2</sup> sensor to compare TAMU<sup>2</sup> with the SeaBeam system, which is an International Hydrographic Office standard bathymetric mapping tool. Imagery and bathymetry data sets that are not coregistered should not be used for detailed studies.

## Acknowledgments

---

This project was funded by Program Element 0602435N, under the direction of Dr. Budd Adams, program manager. The mention of commercial products or the use of company names does not in any way imply endorsement by the U.S. Navy or NOARL.

Finally, we thank Ms. Maria Kalcic and Mr. Jerry Landrum for their technical guidance.

# Contents

---

<b>1.0 Introduction</b>	<b>1</b>
<b>2.0 GLORIA</b>	<b>1</b>
<b>3.0 TAMU<sup>2</sup></b>	<b>2</b>
<b>4.0 Exclusive Economic Zone Survey Experiment</b>	<b>2</b>
<b>5.0 NOARL Image Analysis Techniques</b>	<b>3</b>
5.1 Histogram	3
5.2 Histogram Equalization	3
5.3 Wire-Frame Mesh Vector Plot Projection	6
5.4 Other Enhancement Techniques	6
<b>6.0 NOARL Geological Interpretations</b>	<b>10</b>
<b>7.0 Conclusions and Recommendations</b>	<b>15</b>
<b>8.0 References</b>	<b>16</b>
<b>Appendix A. Current Bathymetric and Acoustic Imagery Sensors</b>	<b>17</b>
<b>Appendix B. Geometric/Radiometric Corrections and Mosaicking of GLORIA Imagery from the Exclusive Economic Zone Survey Equipment</b>	<b>21</b>

# Investigations of Digital Image Analysis and Enhancements of GLORIA Acoustic Imagery

---

## 1.0 Introduction

The U.S. Navy is interested in improving underwater mapping and interpretation technologies for bottom and subbottom segmentation and classification, as well as feature extraction and identification of potential hazards. These refinements would greatly enhance Navy sensors and systems to distinguish and identify underwater objects and the geological structure of the bottom and subbottom.

Before 1970, the Navy could not automatically generate in situ bathymetric contours or acoustic imagery of the seafloor. During the 1970s, multibeam echo-sounding systems began to be developed. This new technology provided the real-time generation of bathymetric contours of the seafloor as a survey ship moved along a given track. Since then, improvements have provided a realistic way to obtain the data required for several naval initiatives. Today, the primary technologies for underwater mapping are the sidescan sonar and multibeam bathymetry sensors.

The Mapping, Charting, and Geodesy Division, Naval Ocean Research and Development Activity\*, was tasked to analyze imagery from the U.S. Geological Survey's (USGS) Exclusive Economic Zone Survey Experiment (EEZ). Digitally mosaicked GLORIA (Geological Long-Range Inclined Asdic) acoustic imagery were analyzed as a zeroth-order model for the acoustic imagery sensor, TAMU<sup>2</sup>, developed by Texas A&M University. Multiple image analysis techniques, as well as several image enhancement techniques, were applied to the data set. Information gained from the analyses will be used in the exploitation of TAMU<sup>2</sup> imagery and bathymetry, when available, for U.S. Navy applications.

This report describes the systems, the USGS experiment, and the methods NOARL used to analyze the GLORIA data. Geological interpretations are provided. The acoustic interpretations will be detailed in a future report.

Appendix A provides details of attributes of the current sidescan/bathymetry sensors of choice. The section on SeaBeam should be particularly noted because it is one of the International Hydrographic Office's standard bathymetric mapping sensors. Appendix B describes the USGS geometric and radiometric correction techniques using their mini-image processing system.

## 2.0 GLORIA

The GLORIA system is a long-range sidescan sonar sensor developed by the British Naval Institute of Oceanography at Wormley. GLORIA was developed specifically to map the morphology and texture of seafloor features in the deep ocean.

The sidescan vehicle (towfish) for GLORIA is 8 m long, weighs 2.25 tons in air, and is almost neutrally buoyant. The sonar arrays consist of 120 transducers, 30 to a row, 60 to each side. The vehicle is towed about 400 m behind the ship with no active depth control, but at the normal survey speed of 8 kt. Vehicle depth is 50 m.

GLORIA's operating frequency is approximately 6.5 kHz, with the port array at 6.8 kHz and the starboard array at 6.2 kHz to eliminate cross-talk between the two sides. Each array is 5.3 m long by 40 cm high; this configuration gives a horizontal acoustic beam 2.7° wide and a vertical beam of 35°. The beamwidth is specified between half-power points, and considerable energy radiates outside these limits. The arrays are designed to confine the energy as nearly as possible to the plane perpendicular to the track and to fill the quadrant from nadir up to near horizontal.

The maximum swath width depends mainly on the prevailing acoustic propagation conditions of the water column. For GLORIA, the swath width can be as wide as 30 km on each side of the track. Normally, however, it is usually somewhat less.

The acoustic backscatter energy is reflected from the seafloor and is recorded digitally on magnetic tape. Each pixel of the image has an along-track size that

---

\*Recently designated the Naval Oceanographic and Atmospheric Research Laboratory (NOARL).

Characteristics of popular side-scan/bathymetry sensors.

SYSTEM	GLORIA	SWATHMAP	SEAMARC II	SEAMARC I	SEABEAM	DEEP TOW
Frequency (kHz)	P 6.5, S 6.7	3.5	P 11, S 12	P 27, S 30	12.158	110
	FM Sweep	FM Sweep	CW	CW	CW	CW
Pulse Length $\tau$	2, 4 sec		25-10 ms	15-3.2 ms	7 ms	2, 5 ms
Pulse Rep. (sec)	20-40	40-48	1, 2, 4, 8, 16	5, 1, 2 or 4	1-22	1
Bandwidth $\omega$	100 Hz		2 kHz-100 kHz	5 kHz-200 kHz	225 kHz	10 kHz
Beamwidth (deg) $\theta, \Phi$	2.7, 30		2, 40	1.7, 50	T 2.7, 54 R 16(20, 2.7)	.75, 60
Cross-Track Resolution $\Delta R$	20 m		5 m	.5 m		.15 m
Tow      Depth D Altitude H	30-60 m	Hull Mount	50-100 m	up to 6 km	Hull Mount	up to 7.5 km
				12-1250 m		10-100 m
Horizontal Range (km) R	15-30	up to 36	.5, 1, 2.5, 5	.25, .5, 1, 2.5	3/8 Water Depth	.5
Speed (kt)	up to 11	up to 20	up to 10	1-3	up to 15	1-2
Array      Length (m) Width (m)	5.33		3.8	1.5	T 2.8, R 2.8	1.25
	18		.2	.2	T .16, R .4	.08
Vehicle      Length (m) Width (m)	7.75		5.5	3		2
	.8		1.3	1.2		.7

is proportional to the range. The size increases hundreds of meters at extreme range because the sound beam diverges at  $2.7^\circ$ . The recording system was designed so that one complete scan is subdivided into 1000 pixels. The cross-range pixel size represents about 50 m, which is smaller than the along-track pixel size. Thus, features in the raw data are elongated parallel to the track, particularly at extreme ranges. GLORIA's characteristics are shown below relative to other popular sensors in the table.

### 3.0 TAMU<sup>2</sup>

(The following describes the TAMU<sup>2</sup> design, since the actual system was not completed at the writing of this report.)

This system is a towed, multispectral, bilateral imaging sonar. TAMU<sup>2</sup> is capable of simultaneously generating, in real time, ship-speed-corrected and slant-range-corrected acoustic backscatter images. It can also generate matching, color-encoded bathymetric charts of the seafloor.

TAMU<sup>2</sup> uses multifrequency operation, where the system provides extremely wide operational limits: swath widths from 200 m to 20 km, operating depths from 20 m to 500 m, operating altitudes from 20 m to 11 km, and tow speeds from 1 kt to 10 kt, depending on the mode of operation.

TAMU<sup>2</sup> has four primary sensor systems:

- The long-range bilateral imaging sonar operates at 11 kHz and 12 kHz and is capable of making bathymetric measurements.

- The high-resolution bilateral imaging sonar operates at 72 kHz and is capable of making bathymetric measurements.

- The towfish environmental sensors measure depth, pitch, roll, and heading of the towfish, as well as the conductivity and water temperature.

- The three-component magnetometer.

The towfish is slightly buoyant and is towed behind a dead-weight depressor. This configuration provides excellent towfish stability under a wide range of sea conditions.

Note: In shallow water the TAMU<sup>2</sup> system can record raw and processed data from both the 72- and 12-kHz transducers. Processed data is primarily defined as imagery and bathymetry that has been "binned" or pixelized (1000 pixels per side).

### 4.0 Exclusive Economic Zone Survey Experiment

The USGS has performed valuable research using the GLORIA sensor for compiling digital mosaics and the radiometric and geometric correction of the GLORIA imagery. They designed and wrote expanded software to process digital images from GLORIA. They also separated the software into two broad categories: preprocessing and analysis/information extraction. The various products show, often for the first time, detailed information used to map the seafloor. These maps give a large overview of a region, similar to regional views of land areas that are provided by Landsat's multispectral scanner images. These maps help to identify areas that may be



hazardous or need further study. This software is part of the USGS Mini-Image Processing System—MIPS (see App. B).

An atlas with acoustic imagery (sonographs) of parts of the Gulf of Mexico was produced by the USGS using imagery collected during the EEZ. Many image processing techniques were used to enhance this imagery. Those produced by the GLORIA sensor represent the backscatter of the seafloor produced by the 6.5-kHz frequency. The strength of the acoustic backscatter is a function of seafloor and water column properties, in particular,

- slope angle of a feature relative to the incident sonar signal (topographic characteristics);
- seafloor roughness factor (the minimum is 4 cm of relief for the GLORIA system, determined by the wavelength of the sonar and the grazing angle of the sonar ray to the seafloor);
- variation in physical properties of the upper few tens of centimeters of the seafloor (distance that attenuates sonar signal strength, as well as produces background noise).

USGS recorded the backscatter as an intensity value; the range of 0 to 255 intensity values (8-bit data were generated from an acoustic pulse every 30 seconds to give a maximum range of 22.5 km on each side of the ship's track). The reflected sound waves were time-recorded so that the data were in a slant-range rather than a ground-range (true geographic) geometry. Also, variations in the ship's speed generated variations in the pixel size of the footprint (the composite imagery) in the along-track direction. These and other distortions were corrected so that the sonographs represented orthorectified and true plan views (assuming a flat seafloor) of acoustic backscatter on the seafloor.

After gathering the data needed to form their atlas, the USGS performed major geometric and radiometric corrections, as well as digital mosaicking. All software corrections were performed using the MIPS, which allows the USGS to have an office or a laboratory image-processing environment that can also be used in the field. See Appendix B for details of these procedures.

## 5.0 NOARL Image Analysis Techniques

The GLORIA mosaicked imagery was used as a zeroth-order model for future (TAMU<sup>2</sup>), more complex data sets.

The following techniques were applied to the GLORIA mosaicked acoustic imagery with the

motivation of finding a probability distribution function estimator and identifying geological areas that need more detailed interpretation and feature extraction.

Multiple techniques were also applied to the GLORIA imagery to deduce proper kernel/window sizes, filters, and mosaicking techniques that would be the most effective on this type of data. The following image processing techniques were applied to the acoustic imagery data set in this section (GLORIA acoustic imagery): histogram, histogram equalization, and wire-frame vector plot projection.

First, a standard histogram was calculated to provide the first quantitative analysis of this imagery. Next, the histogram was equalized using a standard histogram equalization technique. (Note: acoustic imagery is monochrome.) The Gould DeAnza image processor was used in concert with a Digital Corporation VAX 11/780 computer. The Gould Library of Image Processing Software (LIPS) was used for fundamental image processing functions.

### 5.1 Histogram

Figure 1 shows a sample of GLORIA acoustic imagery taken from the EEZ. The image histogram indicates that this type of imagery has a basically Gaussian distribution of intensity values. Note that these intensity values are 8-bit values; i.e., they vary numerically from 0 to 255. Exceptions to the standard Gaussian distribution are seen at approximately the 120 and 255 intensity values. Note also in Figure 1 that two linear features are easily detected directly below the digits "255." These linear features are enhanced in Figure 2. The ship's track, shown by the two "wide" diagonal lines on the image, is also visible. The clutter around the ship's track is a distortion due to slant-range correction. Therefore, the pixels to both sides of nadir contain invalid information.

### 5.2 Histogram Equalization

The Gaussian distribution histogram was then converted to a uniform (approximately) histogram, i.e., or histogram-equalized. Figure 2 shows an equalized histogram plot. The intensities are spread out to yield more contrast in the image. The equalized histogram accents the "relief," shown by the lower intensity values, much more so than raw imagery. Also, the linear features related to Figure 1 were highlighted even more in Figure 2. These linear features are probably artifacts from the digital mosaicking procedures used by the USGS. The relief is barely detectable in Figure 1 but is easily seen in Figure 2.

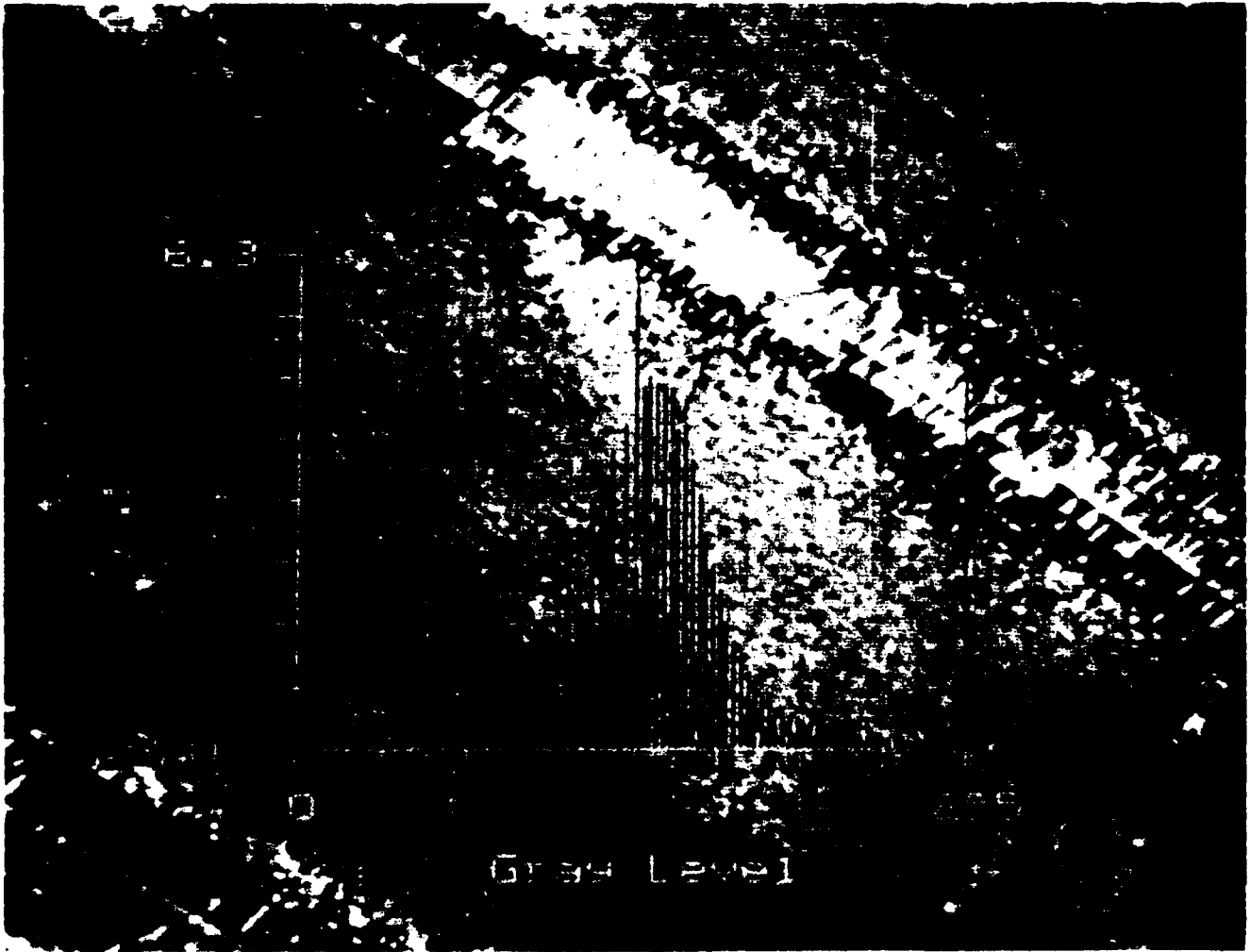


*Figure 1 Histogram of GLORIA imagery*

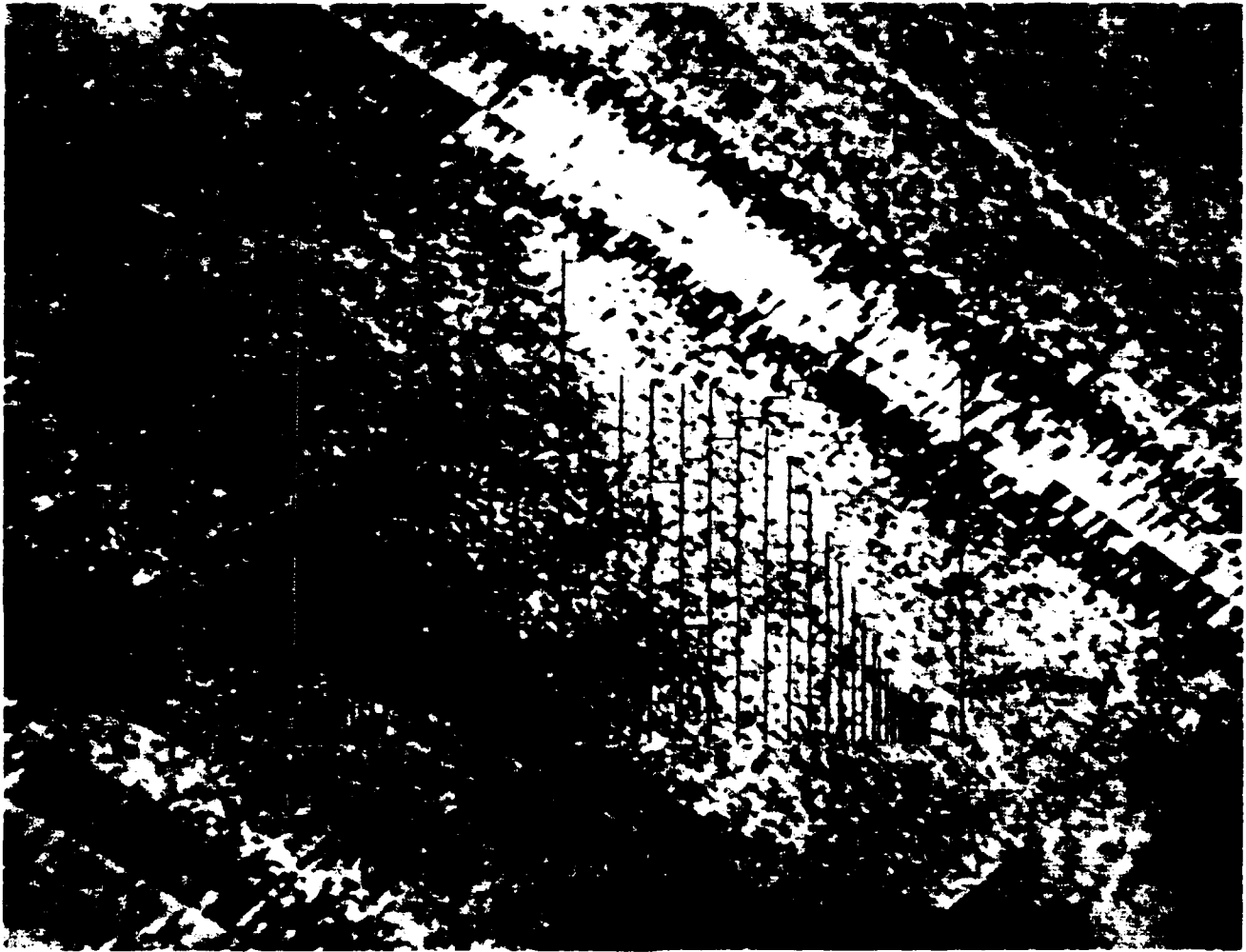


*Figure 2 Histogram equalized GLORIA imagery.*

### 5.3 Wire-Frame Mesh Vector Plot Projection

A "wire-frame" vector plot projection (mesh) of the GLORIA imagery was generated to obtain better interpretation of intensity values and their spatial orientation, as well as their relation to neighborhood pixels. This technique was also used to investigate the possible correlation of intensity values to topographic or bathymetric shape. Figure 3(a) utilized a  $1 \times 1$  sampling size, Figure 3(b) a  $4 \times 4$  sampling size, and Figure 3(c) a  $1 \times 16$  sampling size.

The procedure used in these figures utilized a hidden line technique to produce a wire-frame mesh of the intensity surface of the image. The size and the orientation of the wire-frame mesh can be controlled by adjusting the viewing position coordinates. The size, however, also varies with the size of the memory region on the output channel, as the mesh is scaled to fit in the output region. This mesh was, by far, the most computationally intensive task performed in the initial analysis of the acoustic imagery.

These figures suggest that the production of a three-dimensional, "sun-angle," shaded-relief view of this type of imagery would enhance the interpretation of acoustic imagery. (This likelihood is being studied at NOARL.) Also, no correlations could be drawn between intensity values and bathymetry. Finally, note that Figures (a) and (b) are too "busy" for normal visual interpretation, but that figure 3(c) increased the sampling area and provided only the necessary "envelope" variations of the image.

### 5.4 Other Enhancement Techniques

Several digital image enhancement techniques were applied to the acoustic imagery shown in Figure 1. Existing Gaussian, median, difference, gradient, and threshold techniques were investigated, as well as proper kernel-size selection. The kernel, or filter, is usually square. It is crucial to the computational speed of some of these techniques (especially the median filtering routine), as well as to the final image quality. These enhancements can make the difference in whether or not a feature—say, an underwater mine—is detected.

#### 5.4.1 Gaussian Filters

Figure 4 shows the results of applying Gaussian filters with various kernel sizes. The upper left corner contains the original GLORIA image; the top right image is the resulting image after a  $5 \times 5$  Gaussian filter. A kernel size of  $13 \times 13$  has been applied to the lower left image. A  $29 \times 29$  kernel size was used on the lower right.

It is extremely apparent from the Figure 4 images that the kernel size for the Gaussian filter is of paramount importance. In the bottom right image—the  $29 \times 29$  kernel—note that the image has been blurred (the  $13 \times 13$  kernel also introduced some blur). Note also that the  $5 \times 5$  Gaussian kernel did provide some enhancement of the darker "relief" areas, which can be used as a processing stage preceding a possible segmentation/classification algorithm, e.g., for seafloor bottom classification.

#### 5.4.2 Median Filters

In the process of smoothing imagery, the edges or the high-frequency components usually suffer. However, with median filtering, these edges can be preserved throughout the process, given the approximate window size. Figure 5 demonstrates the application of a median filter with varying window size to the image. Shown in Figure 5, upper left and proceeding from left to right and top to bottom (as will be the case for all multiple images), is a  $3 \times 3$  kernel size followed by a  $5 \times 5$ , a  $10 \times 10$ , and a  $16 \times 16$ . The  $5 \times 5$  window size in Figure 5 seems to offer the most promise for enhancing this GLORIA imagery without sacrificing the image's fidelity. The edge-sharpening, by using the proper window-sized median filter will greatly improve feature extraction algorithms used to locate linear objects.

#### 5.4.3 Difference Filters

One way of defining difference ("differences" are approximations for the derivative or gradient operator) operators for edge detection is to fit a polynomial surface to the gray levels about a given pixel and then use the gradient (magnitude and direction) of this polynomial as an estimate of the image gradient. The  $x$  and  $y$  partial derivatives of the polynomial can be expressed directly for neighborhood gray levels so that actual surface fitting is not necessary. For example, if a plane is fit by the least-squares method to a  $2 \times 2$  neighborhood, then the magnitude of the gradient of that plane is the same as the root-mean-square (rms) magnitude of the Roberts operator. The Roberts' gradient is one of the many techniques for estimating differences in digital images and is given by

$$G[f(x,y)] = \{[f(x,y) - f(x+1, y+1)]^2 + [f(x+1, y) - f(x, y+1)]^2\}^{1/2},$$

where  $f(x,y)$  denotes pixel position. More information on these difference estimates can be found in Gonzalez and Wintz (1987).

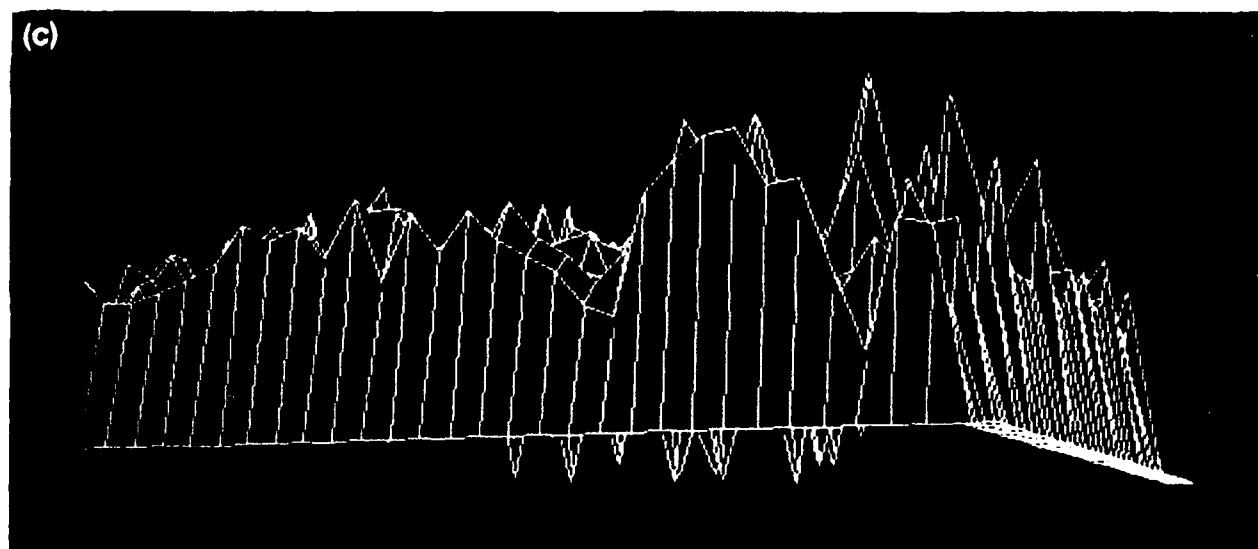
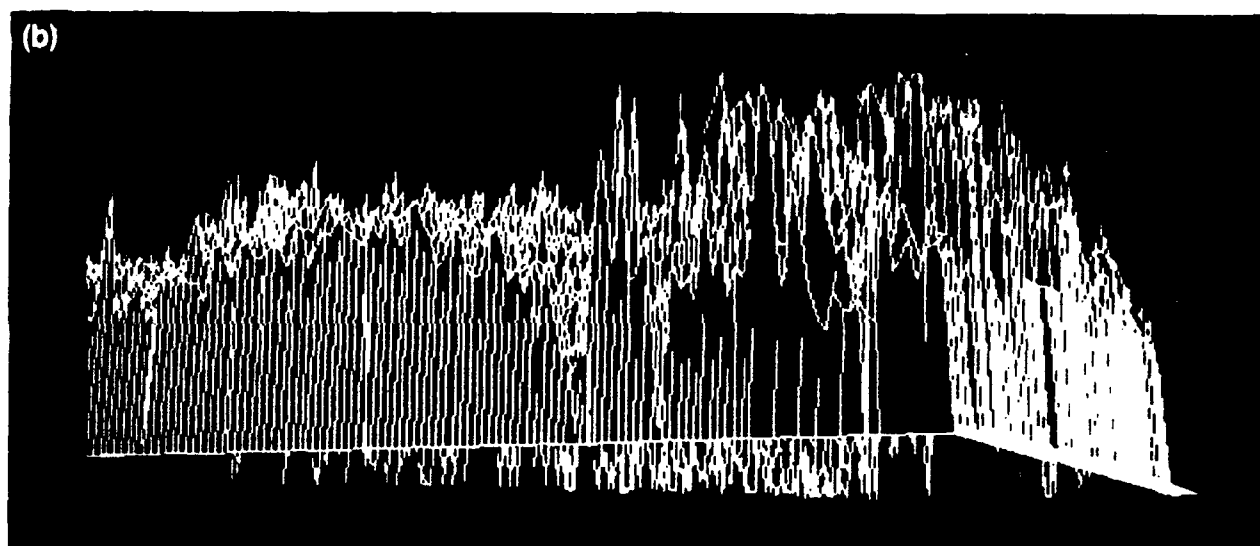
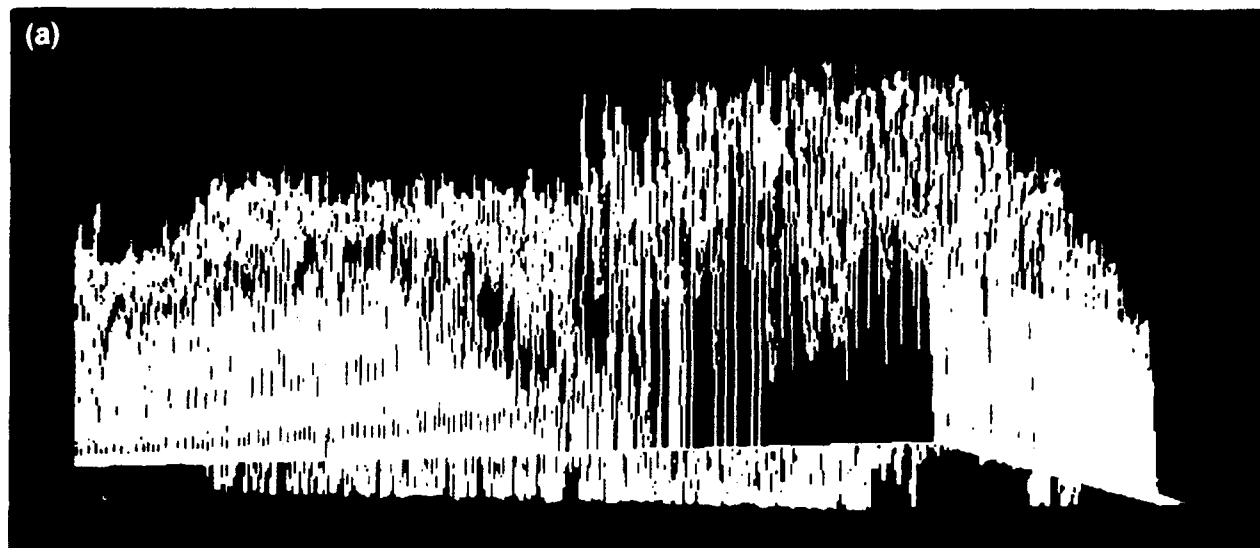


Figure 3 Wire frame intensity plot samplings (a)  $1 \times 1$ , (b)  $1 \times 4$ , and (c)  $16 \times 16$

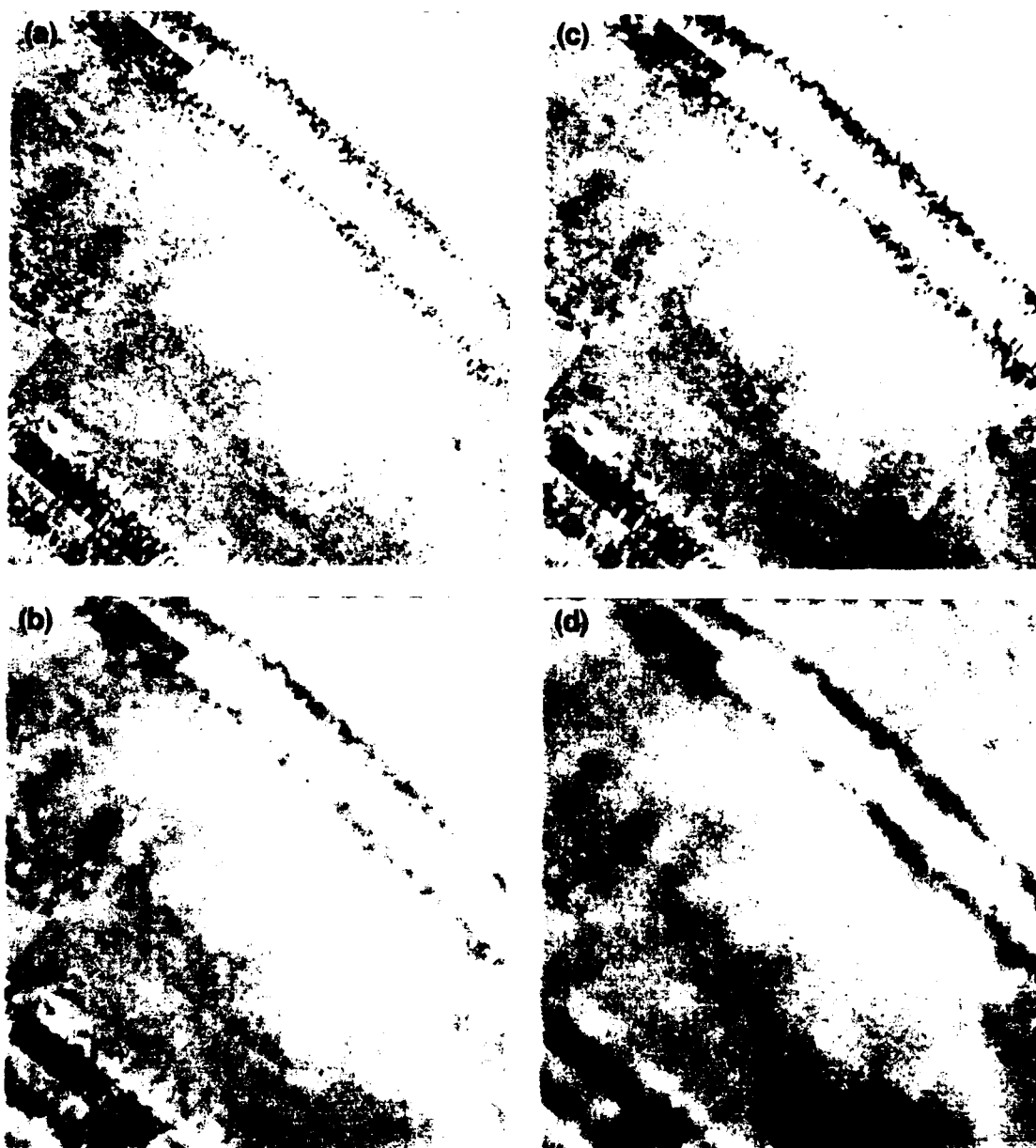


Figure 4. (a) Original GLORIA imagery; (b)  $13 \times 13$  Gaussian filter; (c)  $5 \times 5$  Gaussian filter; and (d)  $29 \times 29$  Gaussian filter

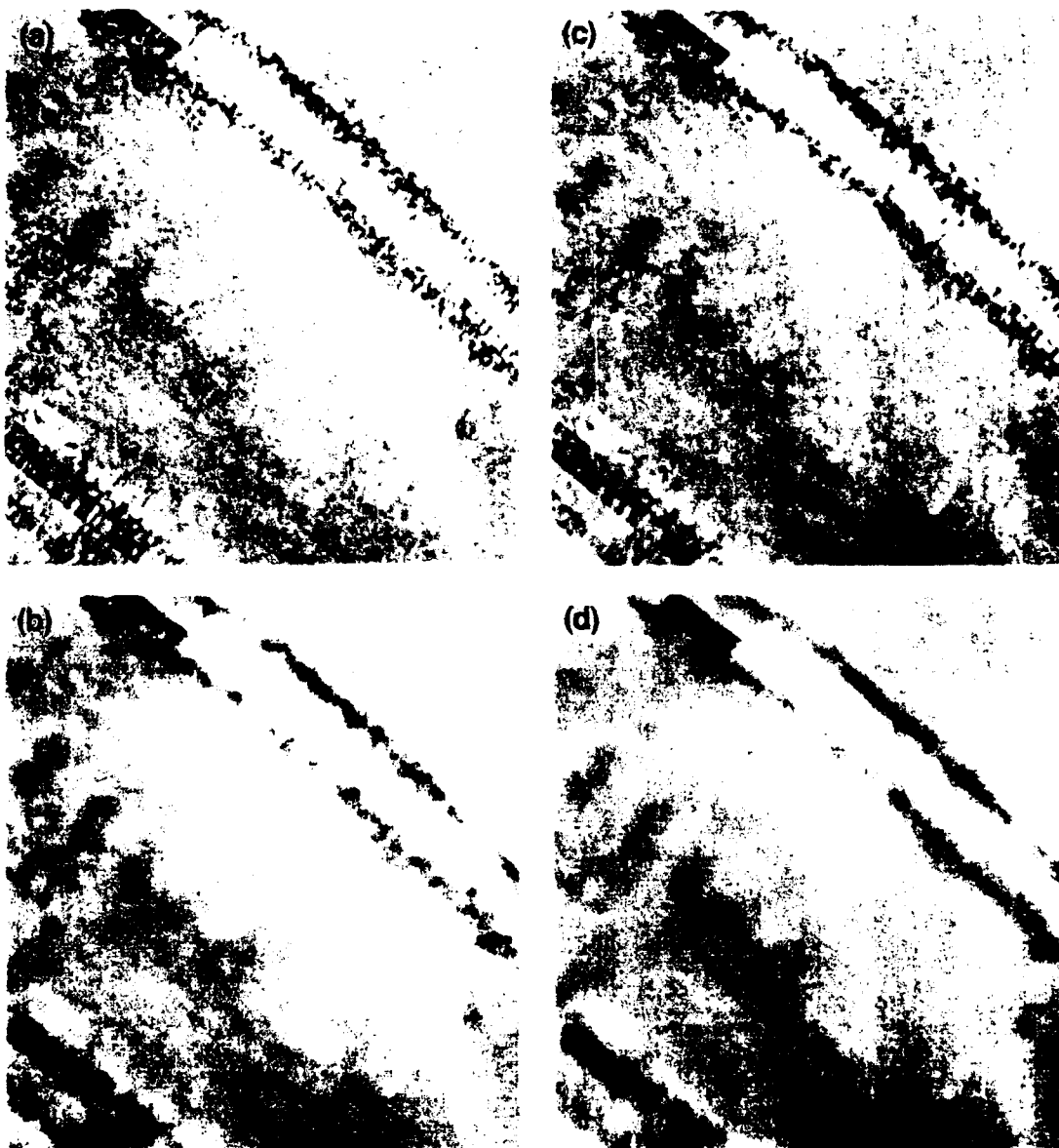


Figure 5 Median filters (a)  $3 \times 3$ , (b)  $10 \times 10$  (c)  $5 \times 5$ ; and (d)  $16 \times 16$

If we fit a quadratic surface to a  $3 \times 3$  neighborhood, the  $x$  and  $y$  partial derivatives are proportional to the results of convolving the image with the Prewitt operator:

$$\begin{array}{ccc} -1 & 0 & 1 \\ -1 & 0 & 1 \\ -1 & 0 & 1 \end{array} \quad \text{and} \quad \begin{array}{ccc} 1 & 1 & 1 \\ 0 & 0 & 0 \\ -1 & -1 & -1 \end{array}$$

Another local feature detection technique (enhancement in the sense that it provides "enhanced detection") is the Sobel operator, defined by convolving the image with the following:

$$\begin{array}{ccc} -1 & 0 & 1 \\ -2 & 0 & 2 \\ -1 & 0 & 1 \end{array} \quad \text{and} \quad \begin{array}{ccc} 1 & 2 & 1 \\ 0 & 0 & 0 \\ -1 & -2 & -1 \end{array}$$

This operator responds to an edge in two positions but is less sensitive to the noise, since it combines differencing across the edge with averaging along the edge (Ekstrom, 1984).

In Figure 6, a horizontal Prewitt filter is applied, followed by a horizontal Sobel, a vertical Prewitt, and a vertical Sobel. Notice the apparent similarities among these images in Figure 6. These difference filters also seem to point to possible bottom texture. This area deserves future pursuit.

#### 5.4.4 Gradient Filters

Figure 7 shows the result of a gradient filter from the directions of north, south, east, and west, respectively. Note that gradient filtering does not perform as well from any direction as the Prewitt and Sobel filtering. Features in Figure 7 have been somewhat concealed because the technique has an intensity reduction effect on this monochrome imagery.

#### 5.4.5 Threshold Filters

Various thresholds within the  $3 \times 3$  neighborhood were utilized in Figure 8 to provide noise removal. The thresholds used in Figure 8 are 4, 8, 32, and 64, respectively. Notice the larger the threshold value, the better definition the interface between the gray and darker intensities.

#### 5.4.6 Vector Intensity Profiles

The Gould LIPS package offers a powerful tool: vector intensity profiling. It allows interactive drawing (with a trackball) of a vector (Fig. 9—red) and then generating of an intensity profile along this vector (Fig. 9—blue). In the first image of this figure, the vector is from the missing section in the middle-left to the upper-right side of the image. In the "missing"

region, USGS filled this area with 127s (midpoint of the 256 dynamic range) to complete this segment. In the second image, the vector runs from upper left to lower right. Notice that the profile along this vector is almost constant. In the third image, the vector runs along the upper ship track. This image profile was an investigation of the transition zone between "real" imagery and the "false," near-nadir imagery. This profile may possibly be used in future work for detecting the boundary between the real and false imagery with the motivation of removing the false. In the final image, the vector is perpendicular to two linear features at the top right corner of the image. These two linear features seem to be artifacts of the mosaicking procedure and could easily be detected, as shown by the peaks in the image profile.

## 6.0 NOARL Geological Interpretations

The unprocessed image in Figure 1 shows a uniform texture with some minor shading. The image is indicative of a compositionally uniform bottom. There is a notable absence of acoustic shadows associated with mounds and ridges, or regions of intense acoustic backscatter from steeply sloping surfaces.

This interpretation is consistent with the location of the image on the lower portion of the Mississippi Cone. The cone is a triangular-shaped wedge of sediment that thickens and narrows toward the mouth of the Mississippi River. Sediment carried by the river is deposited at its mouth and is then transported to the deeper basin, principally by mass movement in the form of debris flows and turbidity currents. These mechanisms tend to produce relatively smooth to low-relief surfaces. Bathymetric contours indicate a gentle regional gradient (less than  $1^\circ$ ). Seismic reflection profiles along the GLORIA track show a smooth bottom with strong, continuous subbottom reflectors (Fig. 2). However, undulation to the bottom is barely perceptible. These undulations could be the cause of the series of the three dark patches that occur (see Fig. 2, left side).

These patches stand out more distinctly in the higher contrast image of Figure 2. Although the processing resulted in a grainier image in Figure 2, the increased contrast improves interpretation and allows several observations. (1) From five to six dark patches are present. (2) The regular spacing of the patches suggests a wave-like pattern, i.e., mudwaves. Because the patches appear to be oriented perpendicular to the GLORIA track (parallel to the beams), the shading



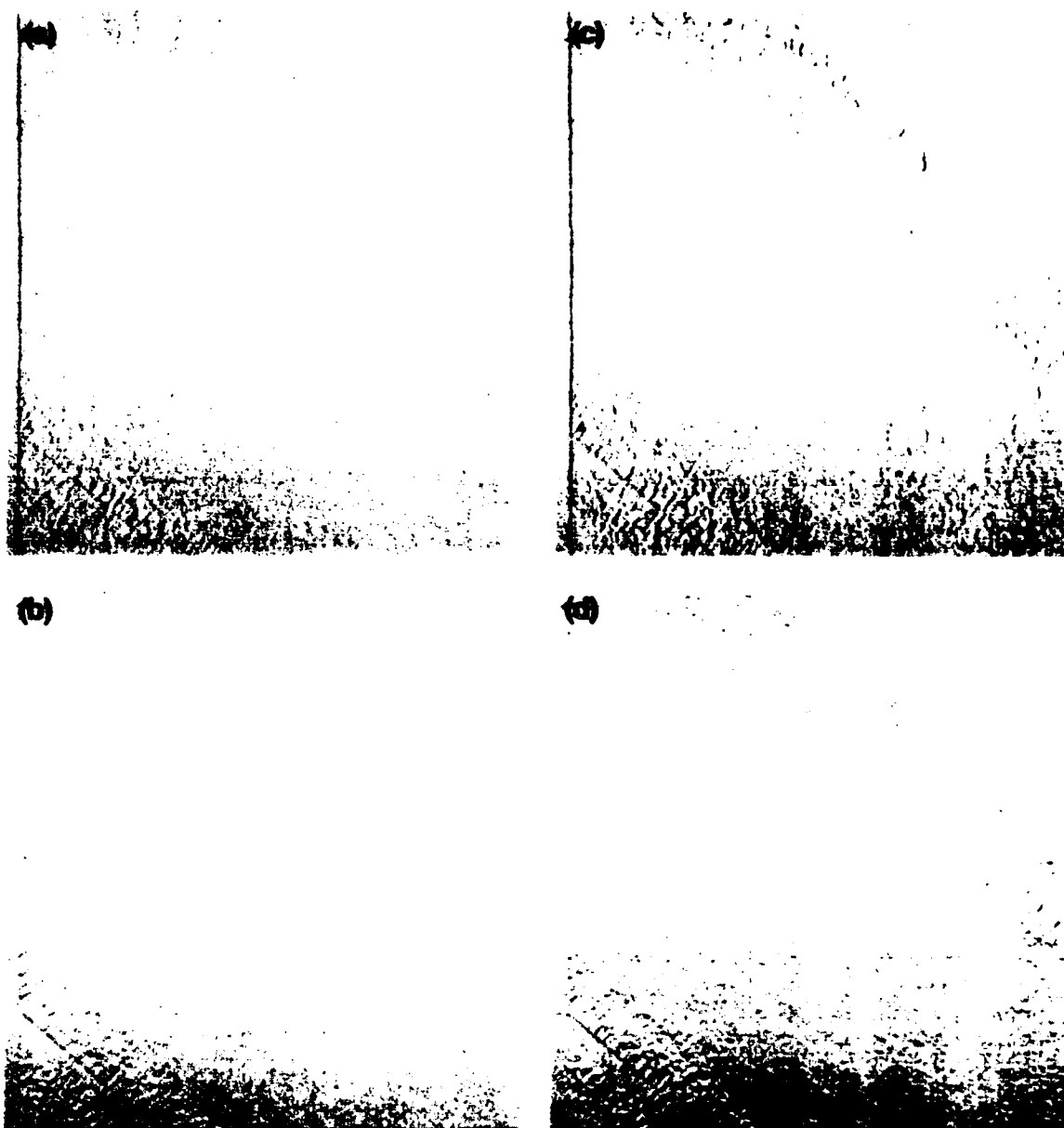
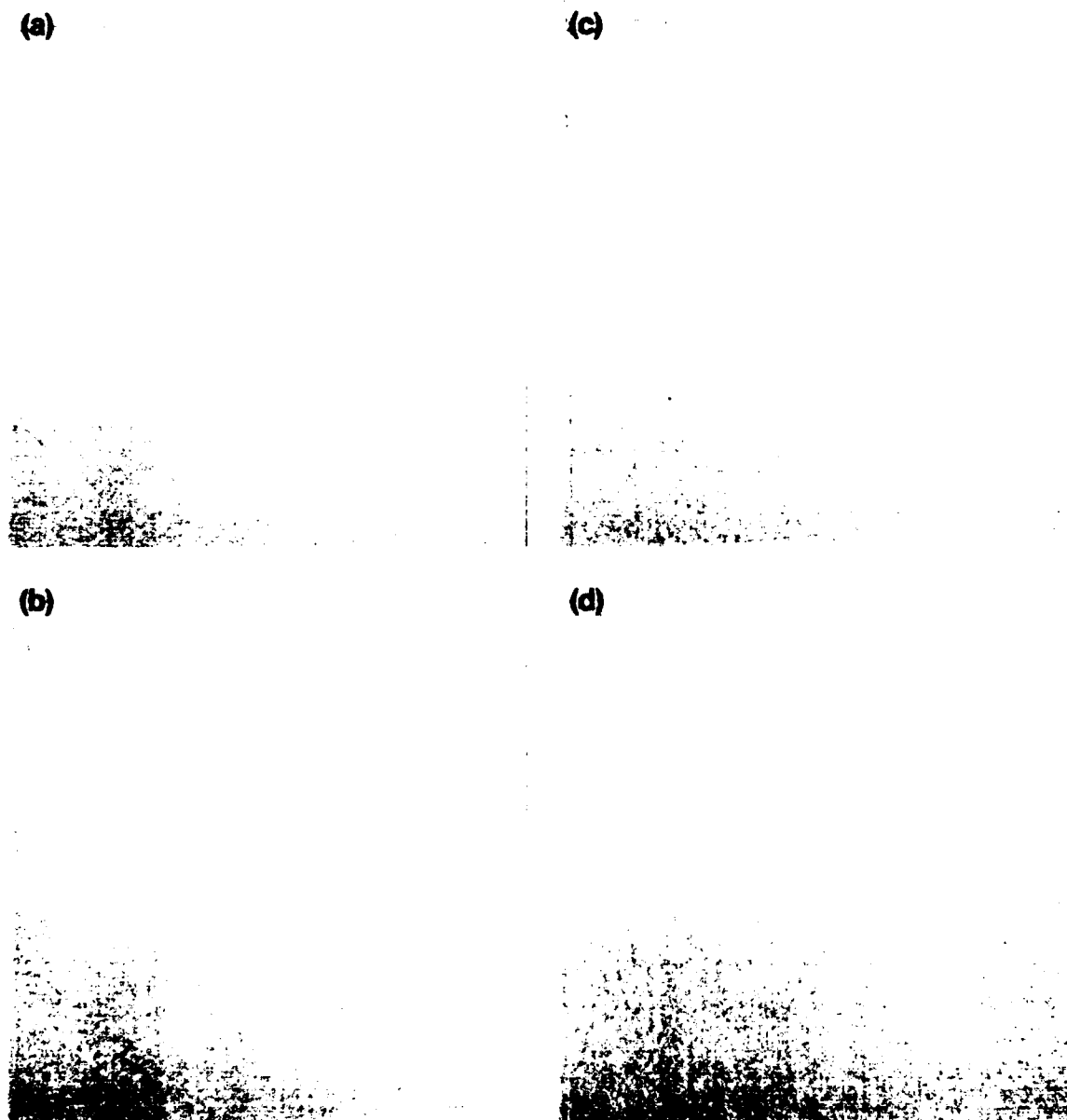


Figure 6. (a) Horizontal Prewitt filter; (b) vertical Prewitt filter, (c) horizontal Sobel filter, and (d) vertical Sobel filter.



*Figure 7. Gradient filters from (a) north, (b) east; (c) south, and (d) west.*

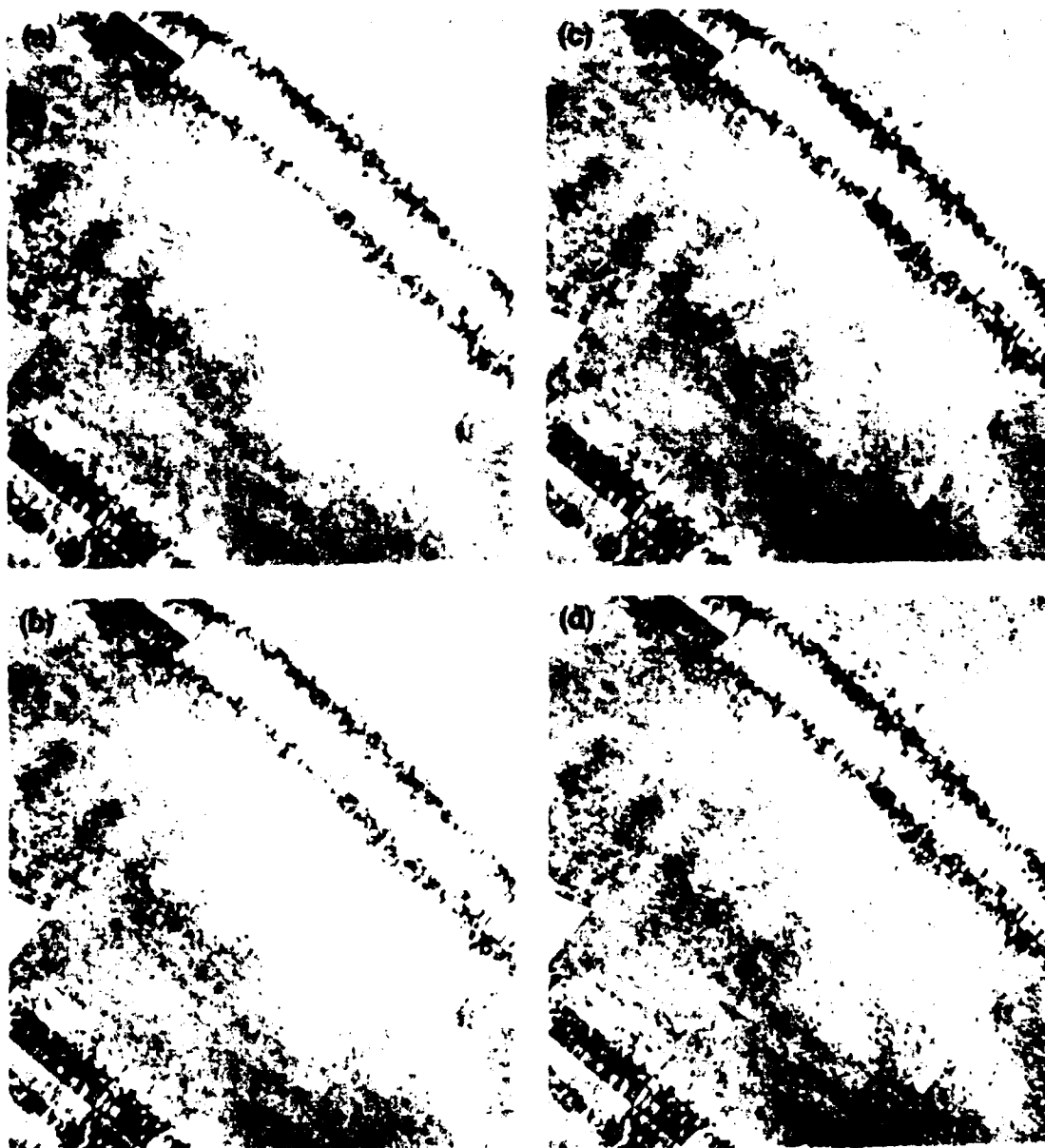
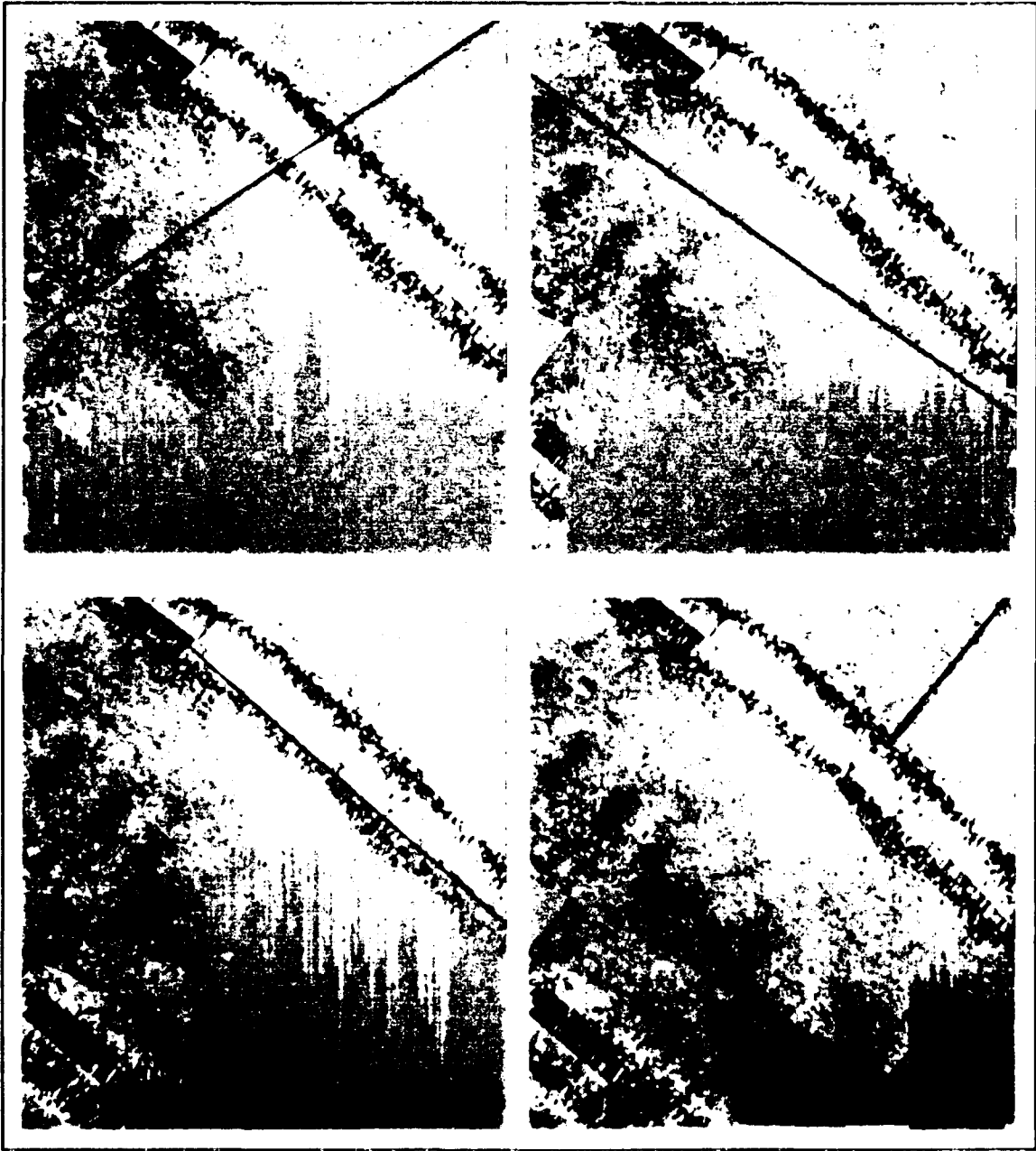


Figure 8.  $3 \times 3$  threshold filters with thresholds of (a) 4; (b) 32; (c) 8, and (d) 64



*Figure 9 Various vector intensity profiles (blue) with respect to different vectors (red) of GLORIA imagery*

could represent sediment textural differences associated with the troughs and crests of the mudwaves rather than actual relief.

Two other features are also highlighted by the increased contrast image of Figure 2. First, a faint difference in shading occurs in the approximate center of Figure 1 (beneath the histogram). In Figure 2, this shading difference has the appearance of a boundary, perhaps associated with some change in sediment texture (e.g., boundary between two debris flows). Second, just below and partially covered by the histogram in Figure 1, the image texture suggests faint northwest-southeast lineations. These lineations are more distinct in Figure 2. Indistinct linearity is also suggested in the upper-right portion of Figure 2 as well.

Because Figure 2 shows an isolated portion of the seafloor, these subtle patterns are not easily interpreted. When viewed in a regional context, however, these patterns are indicative of the sediment dispersal (i.e., flow direction) on the cone and can be interpreted as subtle textural changes and/or low-amplitude relief (subparallel, elongate mounds or furrows) generated by the debris flows and turbidity currents.

It should be noted that the line appearing in the upper-right portion of both Figures 1 and 2 is an artifact of the system. This conclusion is based on the presence of the artifact in other GLORIA images in the Gulf of Mexico and mimics the trend of the GLORIA track. A second point is that some acoustic energy most likely penetrates the sediment/water interface. Therefore, it is possible that some of the subtle patterns seen in Figures 1 and 2 represent shallow buried relief or textural changes of the same type previously described.

The intensity profiles generated in Figure 9 are also useful from an interpretative viewpoint. The relatively constant nature of the intensities along the vectors in the images on the right side of Figure 9 indicates a uniform seafloor with no significant relief or compositional variations. Ignoring those areas where the vector passes over the GLORIA track (useless information), the intensities fluctuate most in the mudwave area (upper-left image), which indicates that this portion of the seafloor and/or subbottom is the most geologically variable.

Based on the previous discussion, it is evident that image enhancement is a useful technique for geological investigations of even relatively bland (geologically speaking) areas of the seafloor. Enhancement of the subtle shading that usually characterizes such areas can highlight features and improve interpretations.

## 7.0 Conclusions and Recommendations

Digitally mosaicked GLORIA acoustic imagery from the USGS EEZ program was analyzed as a zeroth-order model for the state-of-the-art acoustic imagery sensor, TAMU<sup>2</sup>. TAMU<sup>2</sup> imagery and bathymetry were not available for these investigations.

Information gained from this investigation will be used in the exploitation of TAMU<sup>2</sup> imagery and bathymetry for naval applications. Conclusions and lessons learned from the GLORIA investigation are listed. Several recommendations for further study are made.

- Digital mosaicking, i.e., georeferencing, improvements are of prime concern, as evidenced by the number of artifacts present in the GLORIA imagery.

- Histogram equalization yielded vastly improved GLORIA imagery, as far as preparing the imagery for feature extraction and some forms of interpretation. A caution here is that for texture application, which is critical in the segmentation of acoustic imagery, the histogram equalization causes a nonlinear effect that destroys the original texture content of the imagery.

- The probability distribution estimation was found to be close to Gaussian.

- Various sized difference filters enhanced the bottom texture.

- Recommendation: These filters could be used for future segmentation and classification efforts with this type of imagery.

- A direct correlation between bathymetry and the acoustic imagery intensity profile cannot currently be verified due to severe mismatches in resolution of the acoustic imagery and the existing National Ocean Survey bathymetry. Also, this correlation may not exist.

- Recommendation: If a quantitative link between imagery intensity profiles and bathymetry could be established, the more information content could be quantitatively extracted from the acoustical imagery.

- Image analysis offers powerful techniques for allowing the geologist or geophysicist to interpret signatures and structure of the imagery. Histogram equalization, a nonlinear operation that uses the full bandwidth of the intensity range, allowed for improved detection of mudwaves. Also, the intensity profile technique used allowed the geologist to quantitatively view the intensity values along a vector. This capability aided in the detection of the mudwave patterns also in that the intensity fluctuate most in the mudwave area. NOTE: The intensity profile would be even more

useful in an automated scenario where these mudwave area detections would be performed without human interaction.

- Since GLORIA is an (approximately) 6.5 kHz sidescan, returns from the subbottom are present. Therefore, some of the features noted in the GLORIA data set are due to the subbottom. However, the bottom/subbottom boundary components are not well understood.

- Kernel sizes for the various filtering techniques were found to be critical. The  $5 \times 5$  Gaussian filter did provide enhancement of the darker relief areas.

- A median filter ( $5 \times 5$ ) was found to offer edge sharpening without sacrificing image quality.

- Recommendation: This technique could possibly be used in conjunction with feature extraction algorithms to better locate linear objects in acoustical imagery.

- Coregistered bathymetry and imagery are needed for optimum exploitation of bottom information.

- Statistical information for each bin (or pixel) is necessary to develop confidence intervals for each bin

of imagery and bathymetry. Note that this type of statistical information, as well as the coregistered bathymetry/imagery just mentioned, are designed into the new TAMU<sup>2</sup> system.

A final recommendation is that further studies should be conducted with a functional TAMU<sup>2</sup> sensor to compare TAMU<sup>2</sup> with the bathymetry gathered by the International Hydrographic Office's standard, SeaBeam. It is not recommended to use imagery and bathymetry data sets that are not coregistered, e.g., GLORIA and National Ocean Survey.

## 8.0 References

Anonymous (1986). *USGS Atlas of the Exclusive Economic Zone, Western Conterminous United States*, Series I-1792.

Eckstrom, Michael (1984). *Digital Image Processing Techniques*. Academic Press, 1984.

Gonzalez, Rafael and Paul Wintz (1987). *Digital Image Processing*. Addison-Wesley, 2nd ed.

## **Appendix A**

### **Current Bathymetric and Acoustic Imagery Sensors**

---

## SeaBeam

SeaBeam is a hull-mounted, multibeam-swath, echo-sounding system manufactured by the General Instrument Corporation, Westwood, Massachusetts. Its first commercial installation was on the French research vessel, N.O. *Jean Charcot*, in 1977. Since then, SeaBeam systems have been installed world-wide on a variety of ships.

SeaBeam has two groups of transducers installed under the ship's hull. The first group, a 6-m long transmitting array that consists of 20 four-element magnetostrictive transducers is mounted parallel to the keel. The second, a 4-m-long receiving array that consists of 40 piezo-electric hydrophones, is mounted transverse to the ship's keel. The transmitted 12 kHz signal is beamformed by controlling the power and phase of the excitation frequency that is applied to each element of the along-keel array. The signal is then corrected for pitch to produce a stable beam 54° wide across-track and 2.66° fore and aft. The signals are received by the 40 hydrophones and are combined by vector summation to produce 15 "preformed" beams. Each beam is sharply directional; the receive pattern is 2.66° wide across-track by 20° fore and aft.

The composite imagery (footprint) of the transmitted and received beams is 2.66° by 2.66°. Each beam's signal is fed into the echo processor, which calculates the depth and transverse distance from the ship for all beams and all pings. The time interval is limited by the larger slant-range, two-way travel time. The echo processor uses these data to produce a CRT (cathode-ray tube) display of the transverse bathymetric profile and to generate a digital contour plot along the ship's track. The digital contour plots are produced in near real time at a scale and contour interval chosen by the operator. Slope direction is indicated by ticks on alternate contour lines, which are oriented toward increasing depth. Other appropriate annotations are periodically added. Up to 16 pairs of depth and across-track sounding coordinates are externally logged to allow postsurvey processing of the bathymetric data (Davis et al., 1986).

SeaBeam measures the distance between the ship and the first strong reflector in the direction of each of the 16 beams. The true direction of each beam equals the angle of the beam with respect to the ship, plus the mechanical roll angle of the ship at the instant of reception. A digital computer converts the measured slant range and beam direction into true reflector depth and its horizontal distance from the ship's track. Contours of constant depth are computed, based on the 16 depth-distance pairs and are plotted as bathymetric contours with respect to the ship's track.

Although the precision of the system's bathymetric acquisition was improved, the beams are still relatively wide. The single number obtained for each beam's depth is the depth of the nearest reflector in a large area of the bottom. For example, in water that is 5000 m deep, the 2.66° by 2.66° beam insonifies more than 50,000 m<sup>2</sup> of the bottom. The data reduction program assumes the position of the reflector to be in the center of the insonified area. The program computes the depth from the measured slant range as if it were the range to the center. Because the real reflector is seldom located at the center, the precision of the measurement is somewhat misleading. Often, neither true depth nor true position of the reflector is computed—the goal of some surveys is not to determine the precise bathymetry of the bottom, but to learn something about the geology of the bottom (Blackinton, 1986).

## Sea Mapping and Remote Characterization Sensors

The SeaMARC sensors were developed during the early 1970s when mining companies focused on deep-ocean mining, primarily for manganese nodules. An international group, Ocean Management, Inc., developed a deep-towed sidescan sonar, the High Speed Exploration System—HSES ("high speed") referred to the area covered, not to ship speed). The HSES was towed between 100 m and 500 m above the seafloor at a speed of 1 to 2 kt. It produced real-time, true rectilinear (slant range and ship speed corrected) images of the seafloor. The images were 5 km wide and were composed of 2048 gray-scale values (pixel) per ping. Each pixel represented the strength of the echo from a seafloor area that was 2.5 m wide in the athwartship



direction and 2° long in the fore-aft direction. The HSES was a technical success and provided the foundation for the SeaMARC I and II systems.

### SeaMARC I

SeaMARC I, developed by International Submarine Technology, was a deep-towed, bilateral sidescan sonar. It operates at 27 kHz and 30 kHz to produce a real-time rectilinear image that represents a 1-, 2-, or 5-km swath of the seafloor. It emits fan-shaped beams that are 2° wide in the fore-aft direction and 50° wide in the athwartship direction.

The Lamont-Doherty Geological Observatory purchased SeaMARC I in 1980 for use in the search for the Titanic. Although the Titanic was not located at that time, the SeaMARC sensor provided three important improvements to seafloor imaging: the dynamic range of the electronics, a two-body tow system, and enhanced mosaicking capabilities. In the real-time image produced, the water column delay was eliminated, the slant range data were converted to horizontal range, and the along-track dimension was proportional to the speed of the ship. Thus, SeaMARC I images could be mosaicked easily to produce images of large areas that were formerly inaccessible.

### SeaMARC II

The natural progression of this technology led to SeaMARC II, which included a conventional sidescan sonar and a bathymetric mapping system. The higher speed SeaMARC II operates at 12 kHz. This long-range system can be towed in shallow water and will produce a seafloor image up to 10 km wide. In contrast, SeaMARC I operated at 30 kHz and was a deep-towed, slow-speed, sidescan system.

SeaMARC II determines bathymetry by taking measurements 4000 times each second for the magnitude and arrival angle of narrow-band acoustic energy returned from each side of the ship's track. Offline processing of this vector series produces a seafloor bathymetric map along the track, where the width is 3.4 times the water depth. A 10-kt tow capability allows more than 4000 km<sup>2</sup> to be surveyed each day. A key feature of SeaMARC II is the capability to separate the microreflectivity from the macroreflectivity so that the bottom characteristics are better understood.

Bathymetric conversion proceeds three steps. The first step is to examine the magnitude of the arrivals. If an echo magnitude is smaller than that of the noise, then it will be useless in mapping and will be discarded.

The second step is a comparison of the magnitude of the two rows in each array. If the two rows hear the same echo, then they will produce identical output signals. If the two magnitudes differ, then the sample will be discarded.

The remaining samples have an interesting property, called "glissando." Glissando is a series of linear changes in phase. The length of each linear section is roughly the length of the initial acoustic ping. One possible explanation for glissando is that reflections from objects with slightly different ranges will overlap at the arrays and interfere. The resulting phase angle will change smoothly if the amplitudes of the echoes change smoothly.

The third step occurs then the arrival times of the samples remaining after the first two steps (about 10%) are grouped in angle bins. The mean-squared time of all times of all samples in each bin is chosen as the range for the angle at the center of each bin. The electrical angles are converted to acoustical angles by using the map developed during the flat-bottom survey and corrected for the roll of the towfish. The resulting acoustical angle-arrival time pairs are converted to depth and distance from the ship's track. These pairs are assigned geographical positions based on the track of the ship. The positions are interpolated into a grid and contoured to produce bathymetric maps (Blackinton, 1986).

## System Acoustique Remorque

The SAR is a deep-towed acoustic imaging system equipped with different features: a passive depressor, a hydrodynamic vehicle, and an armored coaxial cable. The vehicle is equipped with a bilateral sidescan sonar (170 kHz and 190 kHz) and a mud penetrator (3 kHz to 4 kHz). Other sensors include a long-base acoustic transponder, a depth pressure meter, a magnetic heading, an electromagnetic axis accelerometer, and gyrometers. The shape was designed specifically for improved hydrodynamic stability.

The system produces orthorectified and correlated images in real time and covers 100 m<sup>2</sup> corridors. The average speed is 1 m/sec, which enables a 0.75-m resolution. The output imagery is stored on magnetic tape for further postprocessing. The sidescan sonar identifies reliefs that are on the order of 1-m high and that extend over several meters.

The two sonars are towed near the seabed (about 70 m above) in a towfish with near-neutral buoyancy. Particular care was taken in designing the towfish so that it would remain stable, even in rough sea conditions.

This type of sidescan sonar system is classic; emission and reception take place in a narrow beam perpendicular to the direction of towfish movement. The system's remarkable range and resolution are due to signal processing, high-quality equipment, and digital data transmission.

The mud penetrator emits a conical sonic beam of about 60° below the towfish. The penetrator is outfitted with signal processing facilities and is superior to a ship's depth sounder because it is closer to the seabed.

Although much of the postprocessing software of this sensor was incomplete when the sensor was tested, three key improvements were made after its initial test. Range was increased without affection resolution; the towfish stability was increased, enabling work to proceed in even rougher sea conditions; and the construction of smaller scale, but equally high performance equipment, allowed its use in either shallow or moderate waters (Farcy and Michel, 1985).

## References

- Blackinton, J. G. (1986). *Bathymetric Mapping with SeaMARC II: An Elevation-Angle Measuring Side-Scan Sonar System*. Ph.D. dissertation, University of Hawaii.
- Davis, E. E., R. G. Currie, B. S. Sawyer, and J. G. Kosalos (1986). *Use of Swath Bathymetry and Acoustic Image Mapping Tools in Marine Geoscience*. Geological Survey of Canada, Sidney, BC.
- Farcy, A. and M. Voisset (1985). Acoustic Imagery of the Sea Floor. *Ocean Engineering and the Environment*, Conference Record, vol. 2, p. 1005-1012, San Diego, CA, 12-14 November.

## **Appendix B**

### **Geometric/Radiometric Corrections and Mosaicking of GLORIA Imagery from the Exclusive Economic Zone Survey Experiment**

---

The U.S. Geological Survey (USGS) produced an atlas of acoustic imagery gathered from selected areas of the Gulf of Mexico during the Exclusive Economic Zone Survey Experiment (EEZ). During EEZ, many image processing techniques were used to enhance this imagery. Some of the fundamental image processing techniques are discussed here (McGregor et al., 1986).

### Mini-Image Processing System

All software corrections were performed by the USGS using the MIPS. The thrust of this system was to allow USGS to have an office or a laboratory image processing environment that could also be used in the field. The MIPS was developed on PDP computer hardware with the RSX 11M operating system. MIPS uses Fortran 4+ with some assembly or macroprogramming.

### Geometric Corrections

Major geometric corrections were performed by the USGS due to the effects of the water column offset; the slant-range to ground-range projection; the aspect, or anamorphic, ratio distortion; and the changes in the ship's velocity.

*Water Column Offset.* Because GLORIA records data as soon as it transmits an acoustical wave, the pixels to both sides of nadir contain invalid information. In addition, the true nadir pixels are offset to the sides as a function of the water column or depth. Part of the GLORIA preprocessing software includes merging separate navigation data with the image data. The navigation data are stored in the header section of each line of image data. These data include time and date, latitude and longitude, and bathymetric value at the nadir for the given line. By using the bathymetric value, the sonar image is corrected for the water-depth offset.

*Slant-Range Correction.* The USGS processing software, MIPS (mini-image processing system), recognizes that the GLORIA system collects image data using a near-range depression angle of about  $90^\circ$  and a far-range depression angle of  $5^\circ$  to  $10^\circ$ . The method used to identify a pixel's location in the across-track direction is identical to the method used by side-looking radar imaging systems. Therefore, images with slant-range geometry are generated by the imaging system. The major difference is that most imaging radar systems have a near- to far-range depression angle difference of, at most,  $20^\circ$  to  $30^\circ$ . Because of the extreme depression angle difference, a much more distorted image is created with the GLORIA system; however, the basic geometry characteristics are identical. A linear stretch was applied, as well as pixel enlargement due to the large near-range depression angle (for the pixels near nadir).

Another major geometric distortion present in GLORIA images was the anamorphic ratio present between the along- and across-track directions. The sampling interval in the across-track direction is set up so that the system generates pixels with an approximate resolution of 45 m for a 30-second pulse repetition rate. The MIPS program that corrects for the water depth and the slant-range distortion generates 50-m pixels in the across-track direction. However, the resolution in the along-track direction is determined by the 30-second pulse repetition rate and the ship's velocity. The average resolution in the along-track direction with the 30-second pulse repetition rate is approximately 125 m. This resolution produces images with an aspect ratio distortion of about 2.5 (i.e., 125 m versus 50 m).

Finally, the ship's velocity fluctuations must be corrected. Many variables influence the ship's velocity and cause 7- to 10-kt fluctuations. These fluctuations will cause the pixel resolution in the along-track direction to vary from 110 m to 140 m for a 30-second pulse repetition rate. The distortion is removed by extracting the latitude and longitude from the navigation data and computing the distance traveled by the ship every 30 minutes. Given the distance traveled and the desired pixel size, the number of pixels required for a particular 30-minute segment can be computed.

*Radiometric Corrections.* The second key USGS preprocessing step deals with radiometric corrections. This phase changes the intensity value of a pixel rather than its spatial location, as was the case with the geometric corrections. The radiometric corrections needed for GLORIA

sonar images include (1) shading correction due to power drop-off from near to far range, similar to radar images; (2) shading correction due to a low-power problem at very near nadir due to slow power buildup by the transmitted signal; (3) speckle noise correction; and (4) striping noise removal. These corrections will not be detailed other than to note they were corrected by standard image processing techniques, e.g., pixel averaging and spatial filtering (Chavez, 1986).

## Digital Mosaicking

Past methods were to mosaic strips of images in trackline format into 2° quadrangles. These analog mosaics, while useful for visual analysis, could not use the capabilities of digital image processing to overlay and merge differing digital data sets for analysis and information extraction (Chavez, 1987).

After the sidescan sonar data underwent the initial preprocessing for geometrical and radiometrical correction, the USGS digital mosaicking steps, which would result in the 2° by 2° (or smaller) imagery sheets shown in the USGS atlas, could be performed. The initial processed data segments were approximately 6 hours long. The segments were spliced end-to-end to make a continuous line segment for portions of the trackline where the ship's heading remained generally constant. The segments were tone-matched by adjusting the contrast stretch of each to minimize the seam where they were joined.

Navigation information (latitude and longitude) was determined along the center line of the continuous segment of data at the start, at the end, and at two intermediate points. These four control points have additional pairs of points for each located along the edges of the image. The points were used to position the continuous line segment within the 2° by 2° sheet. After the map projection and latitude boundaries for the sheet were selected, a transformation file was created to position the 12 control points and then the complete image within the sheet.

The next step was to stencil adjacent line segments together to provide a continuous mosaic covering the 2° by 2° sheet. A line was drawn on an interactive terminal video display to outline the portion of each image to be retained. This line was smoothed and then converted from vector to raster format. The rasterized mask was superimposed on the sidescan image. All pixels outside the area of the mask were converted to zero intensity values. This process left only the portion of the image desired. After this stenciling process, each line segment was mosaicked to adjacent segments to sequentially build the composite map. USGS used this process to create a digital file for each 2° by 2° sheet, so the atlas contained all image segments from that particular USGS survey. The scale of the sheets was determined by output of film negatives from a Scitex scanner (McGregor et al. 1986).

A major advantage of digital mosaicking over film mosaicking is that digital mosaicking allows the data to be merged and combined in a quadrangle format with other image and nonimage data sets for digital analysis. In this particular USGS application, the magnetic and bathymetric data, which were collected every 2 minutes at nadir locations during the GLORIA cruise, were merged with the sonar image data. The magnetic and bathymetric data were converted from vector to raster format with the same pixel size and geometric projection as the sonar image mosaic. Then spacial filtering technique was used to interpolate a surface through these data points. Special attention was given to the density and distribution of the data points (high density in the along-track direction and low density in the across-track direction). Last, the resultant image products were then used both individually and with the sonar image data for digital and visual analysis (Chavez et al., 1987).

## References

- Chavez, P., J. Schoonmaker, W. James (1987). Underwater Mapping Using GLORIA and MIPS, *Oceans 87*, Proceedings, Halifax, N.S., September 28-October 1.
- Chavez, P. (1986). Processing techniques for digital sonar images from GLORIA. *Photogrammetric Engineering and Remote Sensing*, 52(8):1133-1145, August.
- McGregor, B. et al. (1986). *USGS EEZ Acoustic Imagery Atlas*, Version 1.0.

# Distribution List

Applied Physics Laboratory  
Johns Hopkins University  
Johns Hopkins Road  
Laurel MD 20707

Applied Physics Laboratory  
University of Washington  
1013 NE 40th St.  
Seattle WA 98105

Applied Research Laboratory  
Pennsylvania State University  
P.O. Box 30  
State College PA 16801

Applied Research Laboratory  
University of Texas at Austin  
P.O. Box 8029  
Austin TX 78713-8029

Assistant Secretary of the Navy  
Research, Development & Acquisition  
Navy Department  
Washington DC 20350-1000

Chief of Naval Operations  
Navy Department  
Washington DC 20350-2000  
Attn: OP-71  
OP-987

Chief of Naval Operations  
Oceanographer of the Navy  
U.S. Naval Observatory  
34th & Massachusetts Ave. NW  
Washington DC 20392-1800  
Attn: OP-096  
OP-96B

David W. Taylor Naval Research Center  
Bethesda MD 20084-5000  
Attn: Commander

Defense Mapping Agency  
Systems Center  
8613 Lee Hwy.  
Fairfax VA 22031-2138  
Attn: Director  
Code SGWN

Fleet Antisub Warfare Tng Ctr-Atl  
Naval Station  
Norfolk VA 23511-6495  
Attn: Commanding Officer

Fleet Numerical Oceanography Center  
Monterey CA 93943-5005  
Attn: Commanding Officer

National Ocean Data Center  
1825 Connecticut Ave., NW  
Universal Bldg. South, Rm. 206  
Washington DC 20235

Naval Air Development Center  
Warminster PA 18974-5000  
Attn: Commander

Naval Air Systems Command HQ  
Washington DC 20361-0001  
Attn: Commander

Naval Civil Engineering Laboratory  
Port Hueneme CA 93043  
Attn: Commanding Officer

Naval Coastal Systems Center  
Panama City FL 32407-5000  
Attn: Commanding Officer

Naval Facilities Engineering  
Command HQ  
200 Stovall St.  
Alexandria VA 22332-2300  
Attn: Commander

Naval Oceanographic Office  
Stennis Space Center MS 39522-5001  
Attn: Commanding Officer

Naval Oceanography Command  
Stennis Space Center MS 39529-5000  
Attn: Commander

Naval Oceanographic & Atmospheric  
Research Laboratory  
Atmospheric Directorate  
Monterey CA 93943-5006  
Attn: Code 400

Naval Oceanographic & Atmospheric  
Research Laboratory  
Stennis Space Center MS 39529-5004  
Attn: Code 100  
Code 105  
Code 115  
Code 125L (10)  
Code 125P  
Code 125EX  
Code 200  
Code 300

Naval Oceanographic & Atmospheric  
Research Laboratory  
Liaison Office  
Crystal Plaza #5, Rm. 802  
2211 Jefferson Davis Hwy.  
Arlington VA 22202-5000  
Attn: B. Farquhar

Naval Ocean Systems Center  
San Diego CA 92152-5000  
Attn: Commander

Naval Postgraduate School  
Monterey CA 93943  
Attn: Superintendent

Naval Research Laboratory  
Washington DC 20375  
Attn: Commanding Officer

Naval Sea Systems Command HQ  
Washington DC 20362-5101  
Attn: Commander

Naval Surface Warfare Detachment  
Silver Spring  
White Oak Laboratory  
10901 New Hampshire Ave.  
Silver Spring MD 20903-5000  
Attn: Officer in Charge  
Library

Naval Surface Warfare Center  
Dahlgren VA 22448-5000  
Attn: Commander

Naval Underwater Systems Center  
Newport RI 02841-5047  
Attn: Commander

Naval Underwater Systems Center Det  
New London Laboratory  
New London CT 06320  
Attn: Officer in Charge

Office of Naval Research  
800 N. Quincy St.  
Arlington VA 22217-5000  
Attn: Code 10D/10P, Dr. E. Silva  
Code 112, Dr. E. Hartwig  
Code 12  
Code 10

Office of Naval Research  
ONR European Office  
Box 39  
FPO New York 09510-0700  
Attn: Commanding Officer

Office of Naval Technology  
800 N. Quincy St.  
Arlington VA 22217-5000  
Attn: Code 20, Dr. P. Selwyn  
Code 228, Dr. M. Briscoe  
Code 234, Dr. C. Votaw

Scripps Institution of Oceanography  
University of California  
P.O. Box 6049  
San Diego CA 92106

Space & Naval Warfare Sys Com  
Director of Navy Laboratories  
SPAWAR 005  
Washington DC 20363-5100

Space and Naval Warfare Sys Com  
4455 Overlook Ave., SW  
Washington DC 20375  
Attn: Commander

Woods Hole Oceanographic Institution  
P.O. Box 32  
Woods Hole MA 02543  
Attn: Director

# REPORT DOCUMENTATION PAGE

Form Approved  
OMB No. 0704-0188

Public reporting burden for this collection of information is estimated to average 1 hour per response, including the time for reviewing instructions, searching existing data sources, gathering and maintaining the data needed, and completing and reviewing the collection of information. Send comments regarding this burden estimate or any other aspect of this collection of information, including suggestions for reducing this burden, to Washington Headquarters Services, Directorate for Information Operations and Reports, 1215 Jefferson Davis Highway, Suite 1204, Arlington, VA 22202-4302, and to the Office of Management and Budget, Paperwork Reduction Project (0704-0188), Washington, DC 20503.

1. Agency Use Only (Leave blank).		2. Report Date. July 1990		3. Report Type and Dates Covered. Final	
4. Title and Subtitle. Investigations of Digital Image Analysis and Enhancements of GLORIA Acoustic Imagery				5. Funding Numbers. Program Element No 0602435N Project No RM35G85 Task No 801 Accession No DN255031	
6. Author(s). Kevin B. Shaw, Charles L. Walker, Steven C. Lingsch, Frederick A. Bowles, and Peter Fleischer					
7. Performing Organization Name(s) and Address(es). Naval Ocean Research and Development Activity Ocean Science Directorate Stennis Space Center, Mississippi 39529-5004				8. Performing Organization Report Number. NORDA Report 247	
9. Sponsoring/Monitoring Agency Name(s) and Address(es).				10. Sponsoring/Monitoring Agency Report Number.	
11. Supplementary Notes.					
12a. Distribution/Availability Statement. Approved for public release; distribution is unlimited. Naval Ocean Research and Development Activity, Stennis Space Center, Mississippi 39529-5004.				12b. Distribution Code.	
<p>13. Abstract (Maximum 200 words).</p> <p>The Mapping, Charting, and Geodesy Division, Naval Ocean Research and Development Activity, was tasked to analyze imagery from the U.S. Geological Survey's Exclusive Economic Zone Survey Experiment. Digitally mosaicked GLORIA (Geological Long-Range Inclined Asdic) acoustic imagery were analyzed as a zeroth-order model for the acoustic imagery sensor, TAMU<sup>2</sup>, developed by Texas A&amp;M University. Multiple image analysis techniques were applied to the data set, as well as several image enhancement techniques. Information gained from the analyses will be used in the exploitation of TAMU<sup>2</sup> imagery and bathymetry for U.S. Navy applications. Technical attributes for acoustic imagery and bathymetric sensors used on current data-gathering systems were also studied and are described in the appendices. This study led to the following conclusions.</p> <ul style="list-style-type: none"> <li>• Improvements in digital mosaicking methods are of prime concern, as evidenced by the number of artifacts located in the USGS GLORIA mosaics.</li> <li>• Histogram equalization yielded vastly improved GLORIA imagery, as far as preparing the imagery for feature extraction and for other forms of interpretation. However, the histogram equalization causes a nonlinear effect on texture application, which is important in segmenting acoustic imagery. This effect destroys the original texture content of the imagery.</li> <li>• The probability distribution estimation was extremely close to Gaussian.</li> <li>• Various-sized difference filters enhanced the bottom texture. The enhancement is useful for future segmentation and classification efforts with this type of imagery.</li> <li>• A direct correlation between bathymetry and the acoustic imagery intensity profile could not be verified because severe mismatches were present in acoustic imagery resolution and the existing National Ocean Survey bathymetry; the correlation might not even exist.</li> <li>• Image analysis offers powerful techniques for allowing a geologist or a geophysicist to interpret signatures and structures of the imagery. Histogram equalization, a nonlinear operation, utilizes the full bandwidth of the intensity range permitted for improved mudwave detection. The intensity profile technique allows the geologist a quantitative view of the intensity values along a vector. This type of view also improves mudwave pattern detection because the intensities fluctuate most in the mudwave area.</li> <li>• Since GLORIA is an (approximately) 6.5-kHz sidescan, there are returns from the seafloor.</li> <li>• Kernel sizes for the various filtering techniques were found to be critical. The 5 x 5 Gaussian filter provided enhancement of the darker relief areas.</li> <li>• A 5 x 5 median filter offered edge-sharpening without sacrificing image quality.</li> </ul> <p>The analyses and conclusions led to these recommendations for study in the following areas.</p> <ul style="list-style-type: none"> <li>• If a quantitative link between imagery intensity profiles and bathymetry could be established, then more information content could be extracted quantitatively from the acoustic imagery.</li> <li>• The intensity profile would be even more useful in an automated scenario where the mudwave area detections would be performed without human interaction.</li> <li>• Coregistered bathymetry and imagery are needed for optimum exploitation of bottom information. Statistical information for each pixel is required to develop confidence intervals for each bin of imagery and bathymetry. Both are designed into the new TAMU<sup>2</sup> system.</li> <li>• Studies should be conducted with a functional TAMU<sup>2</sup> sensor to compare TAMU<sup>2</sup> with the SeaBeam system, which is an International Hydrographic Office standard bathymetric mapping tool. Imagery and bathymetry data sets that are not coregistered should not be used for detailed studies.</li> </ul>					
14. Subject Terms. hydrography, bathymetry, optical properties, tides, reverberation				15. Number of Pages. 28	
				16. Price Code.	
17. Security Classification of Report. Unclassified		18. Security Classification of This Page. Unclassified		19. Security Classification of Abstract. Unclassified	
				20. Limitation of Abstract. None	